Estuarine, Coastal and Shelf Science 292 (2023) 108470

Contents lists available at ScienceDirect

Estuarine, Coastal and Shelf Science

journal homepage: www.elsevier.com/locate/ecss

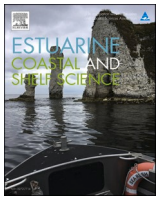

Ecophenotypic variation or genetic differentiation? Ambiguity of morphological and molecular relationships presents uncertainty in host-specific plasticity of *Chelonibia* barnacles

Emily C. Hyatt [a,b,c,*], William K. Hayes [a], Stephen G. Dunbar [a,b,c]

[a] Department of Earth and Biological Sciences, School of Medicine, Loma Linda University, Loma Linda, CA, USA
[b] Protective Turtle Ecology Center for Training, Outreach, and Research, Inc. (ProTECTOR, Inc.), Loma Linda, CA, USA
[c] Marine Research Group, Loma Linda University, Loma Linda, CA, USA

ARTICLE INFO

Keywords:
Commensalism
Epibiosis
Mitochondrial loci
Morphology

ABSTRACT

The genus *Chelonibia*, informally referred to as the turtle barnacles, was historically subdivided into four species by both morphological differentiation and host affinity. More recent studies, however, hypothesized that three of these barnacle species – *C. testudinaria*, *C. manati*, and *C. patula* – comprise a single species, *C. testudinaria*, that exhibits host-specific ecophenotypic plasticity. In this study, we examined both morphological and molecular datasets to assess whether host attachment or genetic differentiation best explains the morphotypes assigned to *C. testudinaria* and *C. manati*. For morphology, we compared 11 mensural test and cirral characters from 71 *C. testudinaria* and 25 *C. manati* specimens identified by the previously established absence or presence of a ridged external dorsal surface. The two morphotypes overlapped in overall body size, although *C. testudinaria* averaged significantly larger and *C. manati* exhibited relatively longer cirri. Discriminant function analyses (DFA) showed strong but incomplete differentiation (92.6% classification success), with one *C. manati* morphotype collected from a sea turtle classified with high confidence as *C. manati*. Thus, the morphological data contradict the host-specificity hypothesis. Genetic analyses using three target loci (16s, 28s, COI) from the mitochondrial and nuclear genomes, as well as a single concatenated sequence of >1600 bp, likewise failed to support genetic differentiation between the two morphotypes within the Atlantic sample. With inclusion of a broader sample of Atlantic *C. testudinaria* and *C. manati* and Pacific *C. testudinaria* barnacles, we found strong population distinction between the ocean basins without morphotype separation. Results of the present study suggest that Balanomorph barnacle taxonomy, especially of endosymbiont species, requires further study, as neither phenotypic plasticity nor genetic differentiation accounted for existence of the two distinct morphotypes.

1. Introduction

Barnacles have been the subjects of a broad range of scientific research, as well as direct commercial use. Barnacles may have been a component of human diets since the Neolithic Age (Dean, 2010), and in Spain and Portugal currently comprise a sustainable, collaborative fishery managed by the European Union (Rivera et al., 2014). In addition, the ability of barnacle larvae to attach to wet surfaces has recently led to investigations of "barnacle cement" in dental research (Newman and Abbott, 1980). Alternately, the true barnacles have long caused problems as fouling organisms on ships and docks, where they add weight and water resistance, and can cause deterioration of submerged surfaces (Holm, 2012). Much study has therefore been devoted to understanding the habits of various barnacle species and seeking out methods to control their settlement and growth. Lack of distinction between species, however, can obscure important variations that have potential for biological, ecological, and economic importance.

Barnacles of the genus *Chelonibia* are obligate epibionts, formerly recognized as four distinct species that differed with respect to both appearance and primary host (Anderson, 1993), until reclassification in 2014 (Zardus et al., 2014). Of the four *Chelonibia* species, *C. caretta* and *C. testudinaria* are primarily found attached to sea turtle hosts (Hayashi et al., 2013; Zardus et al., 2014); *C. patula* is generally associated with crustaceans (Key et al., 1997); and *C. manati* is typically affixed to marine mammals of the Order Sirenia (Hayashi et al., 2013; Mignucci--Giannoni et al., 1999). Recent studies by Cheang et al. (2013) and

* Corresponding author. Department of Earth and Biological Sciences, School of Medicine, Loma Linda University, Loma Linda, CA, USA.
E-mail address: ehyatt@students.llu.edu (E.C. Hyatt).

https://doi.org/10.1016/j.ecss.2023.108470
Received 24 March 2023; Received in revised form 8 August 2023; Accepted 19 August 2023
Available online 26 August 2023

Zardus et al. (2014) used genetic and morphological comparisons to revise the classification scheme, arguing that individuals of *C. patula*, *C. manati*, and *C. testudinaria* all belong to the broad, cosmopolitan species *C. testudinaria* as crab, manatee, and turtle morphotypes, respectively. Cheang et al. (2013) suggested that morphological variation between *C. testudinaria* and *C. patula*, previously considered an indication of speciation, instead represents a manifestation of host-specific phenotypic plasticity in these species. With inclusion of three Atlantic *C. manati* specimens, as well as *C. testudinaria* and *C. patula* from both Atlantic and Pacific locations, Zardus et al. (2014) arrived at a similar conclusion and were able to support the existence of distinct molecular clusters according to the ocean from which they were sourced. These Atlantic and Pacific clades were initially demonstrated by Rawson et al. (2003). Although *C. testudinaria* has replaced *C. patula* and *C. manati* as accepted nomenclature, we hereafter refer to the groups by historic species classification rather than morphotype designation for the sake of simplicity.

Chelonibia spp. often provide refugia for other obligatory and opportunistic epibionts on the carapaces of sea turtles. As this leads to the formation of variable, and often geographically specific, epibiotic communities (Frick and Slay, 2000), monitoring and characterization of community diversity can improve understanding of sea turtle migration and home range analysis (Frick and Pfaller, 2013; Ingels et al., 2020). Barnacles as epibionts can aid in understanding ecology of host species, since interspecific connections, habitat use, and behavior of host species are often influenced by species-specific epibiotic colonization strategies, reproductive modes, and life cycles. An exact characterization of the epibiota present on endangered host species can provide a method for tracing biogeographic ranges and determining the migrations patterns of host species (Ingels et al., 2020; IUCN, 2022). Shahdadi (2023) suggested sea turtle hosts passively facilitate widespread genetic connectivity in disparate populations of *C. testudinaria* across the western Pacific and Persian Gulf. Because populations of all seven species of sea turtles are decreasing globally, prompting IUCN red list levels between vulnerable and critically endangered depending on the species, the use of barnacle species and barnacle clade identities may help us further understand turtle ecology and inform conservation efforts. Likewise, understanding barnacle settlement on other species may inform conservation efforts on their behalf. For example, the West Indian manatee (*Trichechus manatus*) is considered vulnerable (IUCN, 2022), and may similarly benefit from phenotypic plasticity studies.

Phenotypic plasticity comprises the ability of individuals to detect and adapt to external stimuli by altering the phenotypic expression of morphological, physiological, biochemical, or behavioral traits (West-Eberhard, 2003). This flexibility in expression based on environmental cues is typically considered advantageously adaptive, and responsiveness to environmental cues may be an inherent characteristic among living things (West-Eberhard, 2003). Plasticity has been demonstrated in laboratory conditions in many organisms, commonly *Drosophila melanogaster* (Gibert et al., 2004; Karthika et al., 2022; Pétavy et al., 1997; Waddington, 1956), as well as natural populations of New Mexico spadefoot toads (*Spea multiplicata*) (Arendt, 2006), great tits (*Parus major*) (Nussey et al., 2005), and multiple genera of scleractinian corals (Todd, 2008). By definition, phenotypic plasticity characterizes intraindividual modification whereby a single genotype can be expressed as multiple phenotypes (Pfennig et al., 2010), yet has long been postulated as a factor in promoting evolutionary change (Baldwin, 1896). Evidence of genetic assimilation and heritability of plastic traits have been suggested to facilitate adaptive radiation on a rapid scale (Pigliucci et al., 2006; Scheiner and Levis, 2021; Waddington, 1953).

Research demonstrates that the lengths of rami and setae can be influenced by water flow rate and periods of wave action in several intertidal barnacle species, such as *Chthamalus dalli*, *Semibalanus cariosus*, *Pollicipes polymerus*, and *Balanus glandula* (Li and Denny, 2004; Marchinko, 2003; Marchinko and Palmer, 2003). López et al. (2010) determined that reduced wave exposure regimes and lower population densities in the intertidal barnacle *Jehlius cirratus* resulted in longer, thinner cirri, with a corresponding increase in segment number, than those exposed to higher wave exposure and greater population densities. The same report found that *Notochthalamus scabrosus*, another species of intertidal acorn barnacle, showed a similar plastic response to a reduction in wave exposure, but did not change significantly in response to increased population density (López et al., 2010). Nevertheless, phenotypic plasticity in cirral characteristics is not ubiquitous among barnacles, as varying wave exposure conditions did not alter the length of the captorial fan or setae in *Semibalanus balanoides* (Hoch, 2011). Thus, differential morphology observed between *C. testudinaria* and *C. patula* was hypothesized to result from similar mechanisms of plasticity (Cheang et al., 2013).

Settlement on non-host surfaces may provide evidence to refute the host-specific phenotypic plasticity hypothesis, since species-level morphological differences are apparent in several cases in which *Chelonibia* species barnacles have settled on inanimate substrata. Frazier and Margaritoulis (1990) reported an incidence of *C. patula* settlement on a positively buoyant portion of high-density polyethylene plastic in the Mediterranean Sea, with a more recent study suggesting this is not an isolated incident (Sloan et al., 2014). *Chelonibia patula* has recently been documented on inanimate whalebone substrata (Collareta and Bianucci, 2021). Zardus et al. (2014) included a specimen phenotypically identified as *C. patula* collected from a buoy in South Carolina. While no publications have yet reported the settlement of *C. manati* on inanimate materials, this may be due to the species' protrusive basal margin, and consequently its settlement on soft tissue rather than impenetrable substrata (Vallini et al., 2011).

In addition to non-living attachment sites, occurrences of *Chelonibia* spp. on atypical hosts are common in the published literature (Badrudeen, 2000; Monroe and Garrett, 1979; Ross and Jackson, 1972). Nevertheless, Zardus et al. (2014) suggest *C. testudinaria* comprises a broad, cosmopolitan species that attaches to a variety of motile marine animals. Those authors posit that morphological variability (i.e., those characteristics historically used to identify each species) is determined by the host on which the species settles (Zardus et al., 2014). However, *C. patula* has been collected from ornate diamondback terrapins (*Malaclemys terrapin macrospilota*) in brackish and marine estuary habitats in Dixie County, Florida (Ross and Jackson, 1972), as well as from an *Hydrophis cyanocintus* sea snake in the Indian Ocean (Badrudeen, 2000). Moreover, Cintrón-de Jesús (2000) recorded 31 *C. patula* specimens on two Florida manatees (*Trichechus manatus latirostris*). In each of these studies, species identification was based on morphological analysis rather than molecular sequencing.

The preference of *C. manati* to settle on soft-tissue (Vallini et al., 2011) likely prevents its colonization of hard surfaces, such as turtle shells, although the species has been collected from soft tissue along the neck, flippers, and head of hard-shelled sea turtle species (Pilsbry, 1916; Seigel, 1983; Wells, 1966). In addition, the Florida Fish and Wildlife Research Institute (FWRI) maintains specimens that are positively identified as *C. testudinaria* and *C. manati*, respectively, collected from a single green turtle (*Chelonia mydas*) host.

The turtle-specific morphotype phenotypically ascribed to *C. testudinaria* has also been removed from non-turtle hosts. Both the American alligator (*Alligator mississippiensis*) in a coastal estuary of northeastern Florida (Nifong and Frick, 2011) and an estuarine crocodile (*Crocodylus porosus*) in northern Australia (Monroe and Garrett, 1979) have hosted *C. testudinaria* on their keratinized scutes and osteodermal tissue. In the Gulf of Oman, specimens of *C. patula* and distinctly different *C. testudinaria* were collected from individuals of the blue swimming crab, *Portunus segnis* (Shahdadi et al., 2014).

Lack of consistency in association of settlement site and barnacle morphology elicits uncertainty of the presently accepted host-specific phenotypic plasticity hypothesis. Further analyses of *Chelonibia* barnacles are essential to investigate the hypothesis that phenotypic differences among the *C. testudinaria* subspecies represent distinct, species-

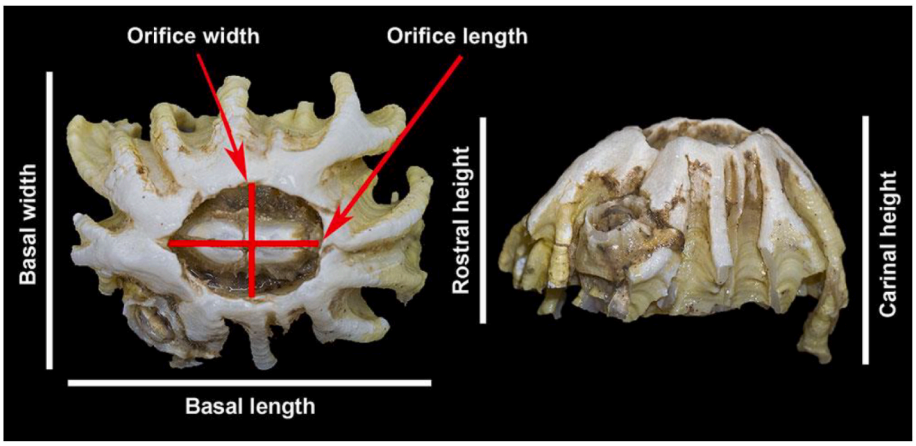

Fig. 1. *Chelonibia manati* specimen CM038 (FWRI) illustrating external test measurements. Due to lack of regularity in the edges of *C. manati* specimens, we measured rostrocarinal (basal) length, basal width, carinal height, and rostral height at the widest margin of the ridges for respective dimensions.

level differences. Here, we explored two sets of hypotheses to better understand whether the morphotypes *C. testudinaria* and *C. manati* correspond to ecophenotypic variation (host-specific attachment) or to genetic clustering. Assuming that morphological traits correspond to host-specific physical environments, we used discriminant function analysis of multiple characters to test whether consistent differences in test and cirral characters exist between *C. testudinaria* and *C. manati*. We also conducted phylogenetic analyses to test whether the two morphotypes cluster genetically and/or geographically between the Atlantic and Pacific oceans.

2. Methods

2.1. Barnacle sourcing

We secured loans of 55 *C. testudinaria*, 16 *C. manati*, and two unidentified *Chelonibia* spp. specimens from the Florida Natural History Museum at the University of Florida (UF) in Gainesville, Florida; 13 *C. testudinaria* from the Yale Peabody Museum (YPM) in New Haven, Connecticut; and three *C. testudinaria* and one *C. manati* from the Florida Fish and Wildlife Research Institute (FWRI) in St. Petersburg, Florida. Twenty-one additional *C. manati* specimens were sent from the United States Geological Survey (USGS) in Gainesville, Florida; and 25 *C. testudinaria* specimens were collected January 13 – February 5, 2020 from *C. mydas* sea turtles and shipped to us from the Sea Turtle Center in Jekyll Island (JI), Georgia. All specimens were collected from hosts permanently residing in the western Atlantic and Caribbean Sea.

2.2. Morphological comparisons

2.2.1. Mensural measurements

All specimens were cleaned of detritus, accumulated algae, and attached epibiota, including non-*Chelonibia* barnacle species. We measured orifice length (ORL), orifice width (ORW), basal length (BL), basal width (BW), carinal height (CAR), and rostral height (ROST) with digital vernier calipers to ± 0.01 mm, following the methods of Jonsson et al. (2018). Orifice length was measured along the rostrocarinal axis, and ORW was measured along the lateral axis (Fig. 1). Unlike *C. testudinaria*, *C. manati* exhibits dorsal extensions used for soft-tissue attachment. Due to this varied dorsal surface, we recorded measurements of basal length, basal width, carinal height, and rostral height at the maximum value of these projections in all specimens (Fig. 1). Among each group, we excluded specimens that lacked sufficiently intact tests for the full set of external shell measurements.

We then derived two more shell measures as bivariate shape ratios from the measures collected. Shell length and height were especially important for calculating elliptical basal area, which has served as a representation of overall body size (Sloan et al., 2014), as well as the conicity and ellipticity of the species. We derived conicity by multiplying the ratios ORL:BL and ORW:BW, and ellipticity by multiplying

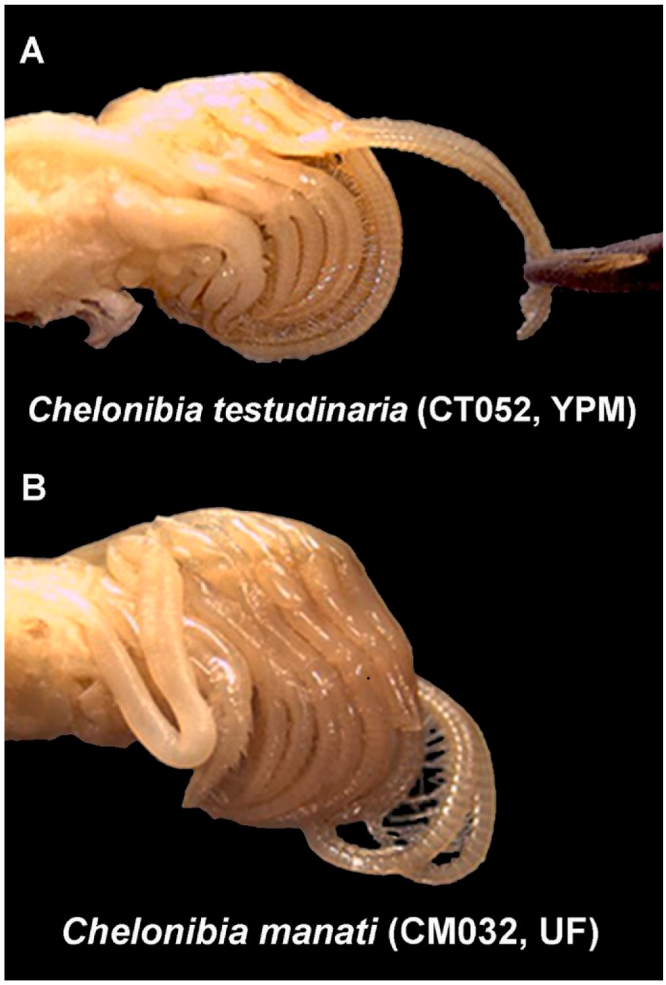

Fig. 2. Representative specimens for dissection microscopy and cirral measurement. (A) *Chelonibia testudinaria* specimen CT052 positioned with paired rami of cirrus IV extended with curved-point needle; (B) *C. manati* specimen CM032 with paired rami of cirrus VI extended.

the two ratios BW:BL and ORW:ORL (Spivey, 1988).

We further collected length measurements of the captorial fan cirri, cirrus pairs IV – VI numbered medial to lateral, as these have classically been used in distinguishing Balanomorph species (Anderson, 1993; Chan et al., 2008; Cheang et al., 2013). Cirral pairs I – III are uniform among the *Chelonibia* barnacles (Anderson, 1993; Cheang et al., 2013), so we excluded them from the current comparison. We used a Leica EZ4 HD dissection microscope with built-in HD imaging and an Acer Aspire E5-575 laptop to capture and record images of barnacles for subsequent analysis with ImageJ software (Schneider et al., 2012). Initial calibration was completed with a clear 4 mm × 4 mm square grid on which the barnacles were placed. We removed barnacle bodies from the shell with a sharp probe and tweezers and blotted the intact soma with paper toweling to dry it. Once dry, cirri IV, V, and VI were located and separated for imagery and measurement. Elongated left cirri were extended outward individually with a sharp probe for image capture (Fig. 2).

In cases where individuals had damaged or absent left cirri, the right side was used, since left and right cirri, as well as posterior and anterior paired rami, are the same length in fully intact specimens (Cheang et al., 2013; Crisp and Southward, 1961; Maciejeski, 2008). One number was recorded for each biramous, mirrored cirral pair. The ramal length was measured as the extended, curvilinear distance along the dorsal margin from base to tip with exclusion of the terminal setae to ±0.01 mm (Geierman, 2007).

Prior to classification analyses, we corrected the nine linear measures (ORL, ORW, BL, BW, CAR, ROST, and the basipod-to-tip-length of the three terminal cirri IV, V, and VI) and ellipticity to control for overall body size. To accomplish this, we obtained the residuals derived from each character regressed separately against the geometric mean of the nine linear measures (i.e., the ninth root of the product of the nine body measurements; Darroch and Mosimann, 1985). Because conicity was independent of body size, we did not adjust it. Geometric mean should be considered the best measure of overall body size (Mosimann, 1970; Mosimann and James, 1979).

2.2.2. Statistical analyses

We conducted three sets of analyses on the morphological data using IBM Statistical Package for the Social Sciences (SPSS) software for Windows, Version 26.0. First, we compared the relative body size of the two morphotypes using the two main measures, basal length and width. Because several outliers were present, we ran nonparametric Mann-Whitney *U* tests, though the results were the same for parametric tests. Second, we compared the relative lengths of cirri IV, V, and VI of the two morphotypes after using basal elliptical area to adjust for body size following Sloan et al. (2014), and again using the residuals from regression against geometric mean, which we consider a better measure of overall body size. We used Mann-Whitney *U* tests for these comparisons, though results were the same for parametric tests. Third, we subjected the 10 size-corrected characters (residuals of nine linear measures and ellipticity) and conicity (11 characters total) to discriminant function analyses (DFAs) to test morphological differentiation between barnacles collected from turtles and manatees. We examined scatterplots to confirm that parametric assumptions of normality, homoscedasticity, and linearity were met, and calculated Mahalanobis distances (Butchart et al., 2010) to screen for multivariate outliers. For DFA models, we relied on SPSS defaults with prior probabilities equal for both groups. We also used leave-one-out classification (a jackknife procedure) for cross-validating the accuracy of group assignments, which reduces bias toward inter-taxon distinctiveness especially with small sample sizes (Lance et al., 2000).

2.3. Genetic analyses

2.3.1. Primer selection

To clarify intra-versus inter-specific differentiation, a narrower primer subset was selected as compared to past studies (Cheang et al., 2013; Zardus et al., 2014). We chose primers based on NCBI BLAST sequence alignment similarity scores with related, non-*Chelonibia* taxa. Based on degree of variation in alignment within *Chelonibia* comparable with that of heterogeneric species, we selected the nuclear, ribosomal loci encoding the 28s and 16s genes as ideal candidates for differentiation. Further, Zhao et al. (2020) suggest that domains of 28s rDNA are useful supplementary loci as an addition to COI for molecular identification of interspecific diversity in mites. We also chose COI due to its status as the *de facto* sequence for species identification and DNA barcoding (Jinbo et al., 2011; Pentinsaari et al., 2016; Trivedi et al., 2016), as well as reflecting the best potential for intrageneric differentiation in Zardus et al. (2014).

2.3.2. DNA extraction

To prepare for dissection, the bench was cleaned with 5% bleach solution (3% hypochlorite) (Prince and Andrus, 1992), which was also used between each sample to clean scalpel, tweezers, and probe to ensure chemical decontamination of surfaces and equipment. We used 5–25 mg of tissue for each specimen, per recommendations of the QIAGEN DNA Fast Tissue Kit, which we selected for use in the current study. For smaller barnacles, the entire body was used to obtain sufficient starting tissue. With larger individuals, the tissue was dissected with emphasis on retaining prosomal tissue, as the anterior scutal-tergal adductor and depressor muscles have previously been established for optimal DNA extraction (Chan et al., 2007; Cheang et al., 2013; Tsang et al., 2008). Once dissected, the tissue was blotted dry and weighed to the nearest mg using a separate weigh boat for each sample to prevent specimen contamination. The weighed and dried tissue were processed according to QIAGEN DNeasy Tissue Kit instructions, and we tested for suitable yield using a NanoDrop 2000 (ThermoScientific). We used resultant values of A260:A280 as indicators of purity for isolated DNA within the solution, and total concentration in ng/μL based on the Beer-Lambert equation (Swinehart, 1962). Ratios of 1.8–2.0 were indicative of pure dsDNA, and we considered app. 100 ng/mL to be the optimal concentration for use in PCR reactions and for subsequent sequencing of the mitochondrial loci.

2.3.3. Polymerase chain reaction (PCR)

We sanitized the hood bench with 5% bleach solution (3% hypochlorite) before preparing each PCR cycle to prevent cross-contamination of genetic material (Prince and Andrus, 1992). Denville Hot Start Taq 2X Mastermix, as well as > 100 ng of eluted DNA was used for each PCR tube based on the specificity of targeting mitochondrial markers (equating to 1–2 μL dependent upon the respective sample DNA yield), combined with 1 μL forward primer, 1 μL reverse primer, and 21–22 μL nuclease free water in respective PCR tubes for a total volume of 50 μL each. Specimens with <50 ng/μL after isolation had concomitantly impure absorbance ratios and were omitted from PCR and further analysis.

We used an MJ Research PTC-200 Gradient Thermal Cycler (MJ Research, Inc.) with 3-min initial denaturation at 94 °C, 36 cycles of 94 °C denaturation for 45 s, 56 °C annealing for 30 s, and a 72 °C extension period of 1 min. After 36 cycles, the tubes were subjected to a final post-elongation period of 10 min at 72 °C, removed from the Thermal Cycler, and placed in a −20 °C freezer for storage.

2.3.4. Gel electrophoresis

We prepared a 7 × 8 cm, 50 mL (1.5%) agarose gel with 1X tris-acetate-EDTA (TAE) buffer for sets of nine PCR products to validate predicted segment length based on primer design, as well as to verify sufficient yield for follow-up sequencing. We prepared each gel such that the first of the 10 1.5-mm lanes was loaded with 5 μL BioLabs 1 kb Plus DNA Ladder to the approximate length of our tested samples. With this Ladder reference, we were also able to determine the concentration of PCR product using the relative fluorescence of the 0.5, 1.0, and 3.0 kb bands as reference for standardized intensity (BioLabs 1 kb Plus provides

length reference bands at intervals between 100 bp – 10 kb). Each subsequent well was loaded with a mixture of 2 μL BioLabs 6X bromophenol blue-based loading dye and 10 μL of PCR product. We ran all gels using a ThermoScientific Owl EasyCast B1A Mini Gel Electrophoresis System at 130 V (60 mA) for 35–40 min in 1X TAE running buffer. We acquired images of completed gels using VisionWorks Software with an AnalytikJena UVP ChemStudio Series CCD camera optimized at 302 nm with Transilluminator UV/blue lighting and EtBr emission filter.

2.3.5. Sequencing

Sequencing was performed by Eton Bioscience, Inc. (San Diego, CA) using an Applied Biosystems 3730xl DNA Analyzer and an Applied Biosystems BigDye Terminator v3.1 Cycle Sequencing Kit for Sanger dye-terminator DNA sequencing by capillary electrophoresis.

2.3.6. Pairwise and multiple sequence alignment

As sequencing was completed with the forward PCR primer for each locus, we used pairwise sequence alignment alongside the reverse primer from the PCR reaction to determine the termination point for each of the received sequences using the European Molecular Biology Open Software Suite (EMBOSS) Needle program (Rice et al., 2000). To verify loci accuracy, the amplified, sequenced region was compared with EMBOSS pairwise sequence alignment against the reference mitochondrial genome (NCBI RefSeq NC_029169.1). The typical Cytochrome Oxidase I site is the approximately 650 base-pair (bp) fragment of the 5′ end of the mitochondrial gene Cytochrome C Oxidase (Folmer et al., 1994). Cross-validations of database sequences were determined to align with the primers that were designed specifically for this study using the NCBI BLAST program.

We attenuated each sequence at the optimal alignment site and standardized sequences based on expected sequence length for the predetermined loci. A Needleman-Wunsch global alignment algorithm (Needleman and Wunsch, 1970) was chosen for alignment optimization, wherein alignment scores are optimized using the edit distance between the two strings (match = 1, mismatch = −1, indel/gap = 0). Global Alignment was chosen over local due to the relative similarity of chosen sequences, as this method spans the entire length of all query sequences rather than assuming greater divergence between them (Polyanovsky et al., 2011).

We used two methods of analysis: a three-gene concatenation approach, in which the gene sequences were concatenated and aligned in 16s-28s-COI order; and a single-gene approach in which each gene was analyzed individually. The single-gene method was further divided into two analyses, the first of which contained only specimens from the present sample, and the second analysis included sequences deposited by Hayashi et al. (2013) and Zardus et al. (2014) in the open source GenBank database (Coordinators, 2015). We designed primers localized for the regions of the *Chelonibia* genome that were sequenced, as opposed to universal arthropod primers chosen by Zardus et al. (2014) and Hayashi et al. (2013), to improve binding precision. We used EMBOSS Needle pairwise alignment to verify precise localization and trim sequences obtained from GenBank for comparable sequence identity. We employed Multiple Sequence Alignment Sequence Comparison by Log-Expectation (MUSCLE) (Edgar, 2004) for alignments with NCBI Clustal Omega (Larkin et al., 2007), incorporating an HHalign algorithm with a profile hidden Markov model (HMM) and default settings for the core alignment engine (Söding, 2005).

We estimated prediction error and relative quality of the statistical model using the Akaike Information Criterion (AIC) where lower AIC indicates better model fit. We used ModelTest software (Posada and Crandall, 1998) for the 28s locus to determine that distance optimization with a Hasegawa-Kishino-Yano (HKY85) nucleotide substitution model (Hasegawa et al., 1985) was optimal for tree evaluation with our data (AIC = 17857.83), and was shown to be preferable to the GTR category (GTRCAT) model used by Hayashi et al. (2013). The latter model, where individual rates are optimized and assigned to rate categories per alignment column (Stamatakis, 2006), is best suited for comparisons among >50 taxa, and therefore generated a poorer model (AIC = 17862.50).

We obtained an initial tree by stepwise addition with 10 random repetitions followed by branch swapping trial rearrangements using a agglomerative clustering Neighbor-joining method (Saitou and Nei, 1987), with the prior distance matrix as the input, to build the final phylogenetic tree in both midpoint-rooted and unrooted formats. The value of kappa (κ) was calculated to determine rate of evolution among loci (Hernandez et al., 2013; Pagel, 1999).

2.3.7. SplitTree5

We performed additional analyses using SplitsTree5 v5.0.0 (Huson and Bryant, 2006), incorporating a NeighborNet method (Bryant and Moulton, 2004) with a BlockPivot algorithm and NNet2021 wt to obtain cyclic splits. The NeighborNet algorithm for constructing phylogenetic networks is based on the neighbor joining algorithm, which similarly employs distance matrices with Kalmanson combinatorial conditions met for arrangement of non-hierarchical, agglomerating clusters, generating non-overlapping splits graphs.

For consolidation of a single, rooted tree with edges and nodes identified, we selected the unweighted pair group method with arithmetic mean (UPGMA) (Huson and Bryant, 2012; Michener and Sokal, 1957) using default options. We combined the Splits Network Algorithm method (Dress and Huson, 2004) with SplitTree5 default options for algorithm design, equal angle convex hull, and Hamming distances to incorporate sequence dissimilarity among groups (Blackburne and Whelan, 2012) and generate a comprehensive, rooted splits network.

2.3.8. BEAST with DensiTree

We prepared data in assembled.xml format using Bayesian Evolutionary Analysis Utility (BEAUti) for processing through Bayesian Evolutionary Analysis Sampling Trees (BEAST) (Suchard et al., 2018). Bayesian methods were used to build informative, precise trees quantifying uncertainty *via* the posterior distributions of parameter estimates. For each algorithm, we used BEAST with a Markov Chain Monte Carlo (MCMC) chain length of 10,000,000 and 10% burn-in; HKY frequency-estimated distance correction; kappa transition-transversion bias set at 1.0; a strict clock model at 1.0 assuming the same rate of evolution for all branches; Yule model tree with uniform birth rate, frequency parameter, and log normal kappa (κ); and the estimated HKY transition-transversion parameter of partition. We ran output data through Tracer MCMC Trace Analysis Tool v1.7.2 to verify that the default chain length of 10,000,000 was adequate for each analysis to produce sufficient independent samples from the posterior distribution for each parameter, as evidenced by an estimated sample size >200 for each statistic (Rambaut et al., 2018).

We processed all output trees with TreeAnnotator v2.6.6, employing a 10% burn-in to find a maximum credibility tree with median heights and the highest possible log clade credibility. DensiTree Tree Set Visualizer version 2.2.7 (Bouckaert and Heled, 2014) was used to illustrate the resultant target tree.

To assess geographic clustering, we ran an additional analysis which incorporated each of our ten COI sequences with the COI sequence data deposited in GenBank by Zardus et al. (2014), comprising 18 *C. testudinaria* specimens from the western Pacific and nine *C. testudinaria* and three *C. manati* from the western Atlantic and Caribbean. The total sample (n = 32 *C. testudinaria*, 8 *C. manati*) was analyzed using the BEAST software package using the methods previously described.

3. Results

3.1. Measurements

We measured 98 barnacles collected from sea turtles and 37 collected

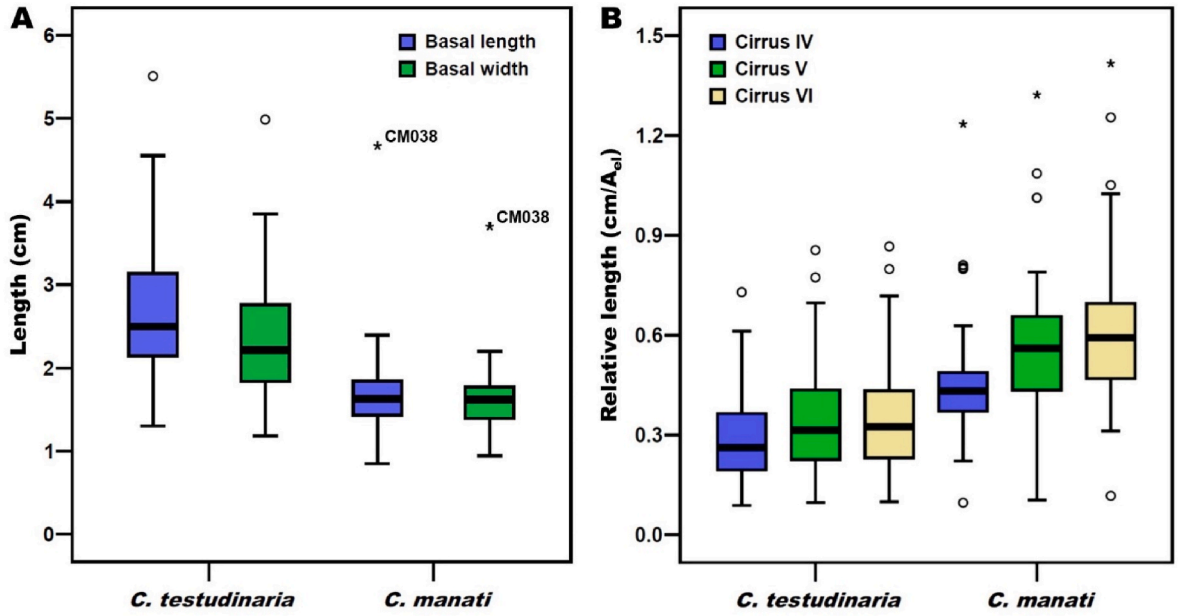

Fig. 3. Box plots illustrating morphological variation of sea turtle (presumably *Chelonibia testudinaria,* n = 71) and manatee (presumably *C. manati*, n = 25) barnacle specimens, including the single *C. manati* morphotype found on a turtle (CM038). (A) Relative body size measures (basal length and basal width). (B) Relative lengths of cirri IV, V, and VI size-corrected for basal elliptical area. Boxes (interquartile range) contain 50% of the values, the horizontal line represents the median, the vertical whiskers show the highest and lowest values excluding outliers, and the circles and asterisks represent outliers.

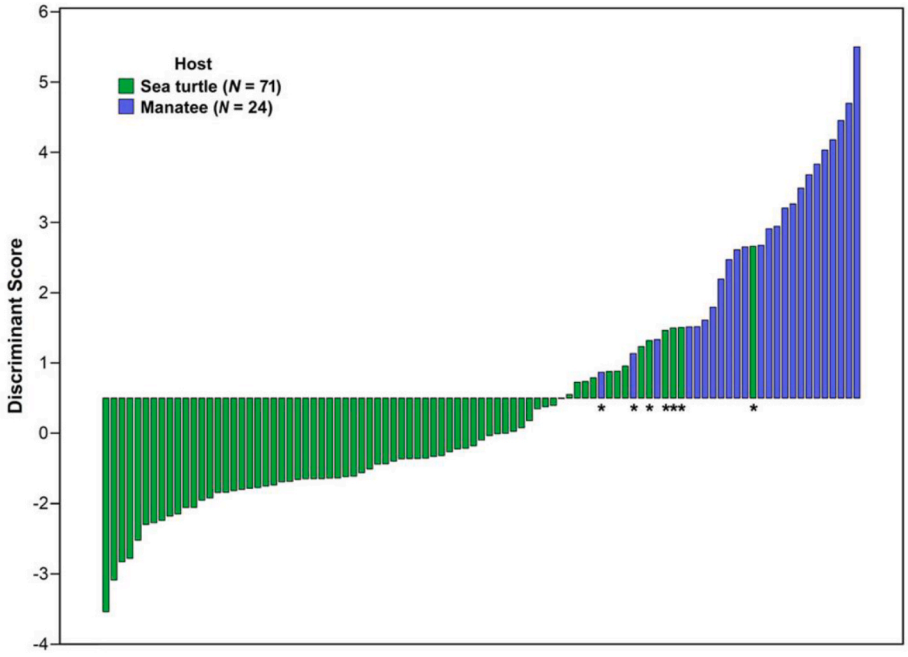

Fig. 4. Classification of barnacles collected from sea turtle (presumably *Chelonibia testudinaria*) and manatee (presumably *C. manati*) hosts via a discriminant function analysis using 11 morphological characters (10 of which were size-corrected). Discriminant scores correspond to degree of differentiation. Overall classification accuracy to host was 92.6% (93.0% for turtle hosts, 91.7% for manatee hosts). Asterisks indicate seven misclassified barnacles. Specimen CM038, a *C. manati* morphotype collected from a turtle, was excluded here but classified as *C. manati* in supplemental models (see text).

from manatees. Of these, 87 from turtles and 33 from manatees had intact shells with all external measurements taken. All but one turtle-derived specimens possessed a relatively smooth external surface typical of *C. testudinaria,* including six that were deemed to be *C. patula* morphotypes based on opercular characteristicss and were excluded from the present study due to the small sample size. The one exception (specimen CM038; Fig. 1) featured the ridged external test surfaces with marked extensions of the shell projecting from the dorsal edge of each shell plate that was present in all manatee specimens and expected of *C. manati*. We further obtained cirral measurements from 71 presumed *C. testudinaria* and 25 presumed *manati* specimens (including CM038). We limited morphological analyses to these 96 specimens with complete data.

The two morphotypes exhibited overlap in overall body size for the two main characters, basal length and width, though *C. testudinaria* was significantly larger for both measures (53.3% greater median length, $Z = 5.46$, $p < 0.001$; 40.0% greater median width, $Z = 4.70$, $p < 0.001$; Fig. 3A). The turtle-derived *manati* specimen (CM038) was the largest of its morphotype. After adjustment for body size using basal elliptical area, relative lengths of all three cirri were significantly greater for *C. manati* compared to *C. testudinaria* (cirrus IV: $Z = 4.27$, $p < 0.001$; cirrus V: $Z = 4.66$, $p < 0.001$; cirrus VI: $Z = 4.90$, $p < 0.001$; Fig. 3B).

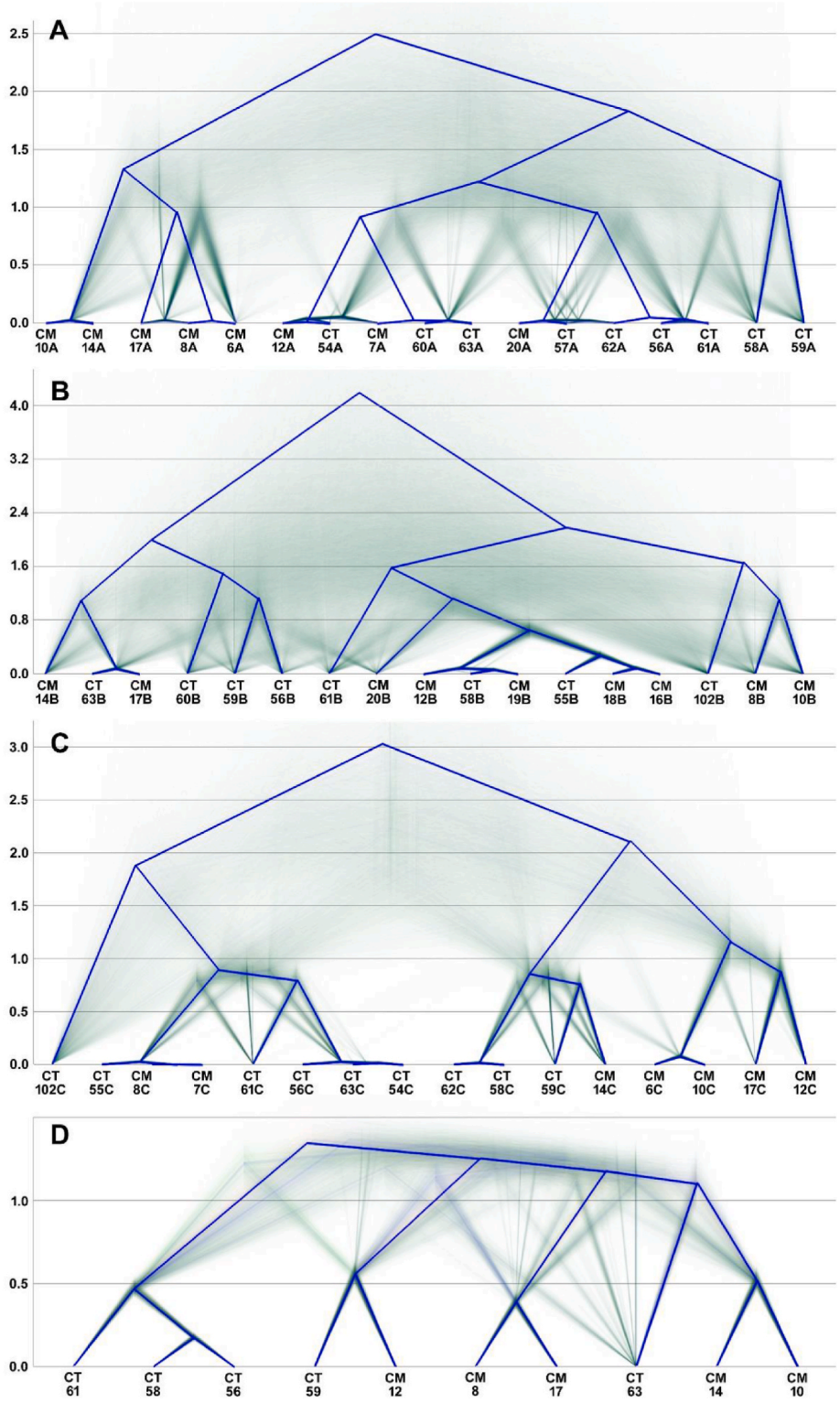

Fig. 5. Top-rooted maximum credibility trees for presumed *Chelonibia testudinaria* (CT) and *C. manati* (CM) sequences generated with DensiTree showing consensus trees (bold lines) and all generated trees with Bayesian hierarchical clustering and tree annotation. Vertical bars represent relative node height. A) 16s with notable uncertainty in node formation; B) 28 s C) COI maximum credibility tree; D) Concatenated sequence with notable uncertainty in node height among higher level splits.

However, when cirri lengths were size-corrected using geometric mean, no differences existed between the two morphotypes (cirrus IV: $Z = 0.40$, $p = 0.69$; cirrus V: $Z = 0.83$, $p = 0.41$; cirrus VI: $Z = 1.13$, $p = 0.26$; data not shown).

3.2. Discriminant function analyses

For the barnacles with complete data, we excluded from analysis the one outlier identified by Mahalanobis distance: barnacle CM038, the *C. manati* morphotype removed from a turtle. The highly significant omnibus DFA that included all 10 size-corrected morphological

characters and conicity ($\Lambda = 0.34$, $\chi^2 = 93.72$, df = 11, $p < 0.001$, canonical $r = 0.81$) successfully classified 92.6% of all specimens (93.0% from turtles, 91.7% from manatees), with five turtle and two manatee specimens misidentified (Fig. 4).

Leave-one-out classification yielded somewhat less success (87.4% overall, 88.7% for turtles, 83.3% for manatees). The best discriminating characters included ROST, cirrus VI, and CAR (standardized coefficients = 0.797, 0.672, and 0.605, respectively). Ratios that included orifice measurements were least effective in discriminating between the two species. Although the model was highly parameterized, a stepwise DFA yielded similar results ($\Lambda = 0.37$, $\chi^2 = 89.84$, df = 4, $p < 0.001$, canonical $r = 0.79$) based on just four characters (cirrus V, CAR, ROST, ellipticity), with 88.4% classification success (97.3% for turtles, 91.7% for manatees).

To assess the identity of barnacle CM038, we added it to DFA models as either a turtle (original host) or a manatee (phenotypic appearance) specimen. When treated as a turtle morphotype, the omnibus and stepwise DFA models identified it as *C. manati* with 95.2% and 100% probability, respectively (overall classification success of models 83.3% and 88.5%, respectively). When treated as a manatee morphotype, both the omnibus and stepwise DFA models identified it as *C. manati* with 100% probability (overall classification success of models 88.5% and 90.6%, respectively).

3.3. Genetic analyses

3.3.1. Tissue lysis and DNA extraction

Chelonibia testudinaria specimen CT102 was chosen at random from Georgia Sea Turtle Center samples for the initial test to determine optimal tissue for standardized methodology. The specimen was bisected into prosoma and cirral portions, each of which was run in a separate extraction procedure. Prosoma tissue weighed 18 mg, while the full mass of the cirral tissue was 9 mg. Poor lysis of the cirral tissue was apparent. We obtained a yield of only 17.5 ng/μL for cirral extraction compared to 185.9 ng/μL isolated from the prosoma. The purity of the DNA was also markedly different, as the prosoma ratio of 1.92 is indicative of pure DNA, while the 2.07 value obtained from cirri suggests impurity in the sample.

Chelonibia manati specimens CM001 – CM004 were collected June 12, 2011, and CM005 was collected June 10, 2012, from Southern Lagoon, Belize, by Cathy Beck (USGS) and stored in 70% ethanol. These specimens had very poor total DNA yield (range 3–25 ng/μL), and were insufficient for subsequent PCR processing, which requires a minimum 100 ng/μL. Further, we obtained absorbance ratios >2.0 for each of the five specimens, indicative of impurity in nucleic acid type.

Additional *C. manati* specimens CM006 – CM010 presented mixed yield results. Specimen CM009 was highly damaged, and the type of tissue was indeterminate. Except for CM007 and CM009, specimens had sufficient mass for prosomal tissue digestion, which was shown to be ideal in the tissue type comparison. Conversely, specimen CM013 was omitted as the total body mass was less than the minimum necessary for lysis, whereas the small size of CM007 necessitated that both prosoma and cirri were used to obtain 8 mg of tissue in order to be within the optimal 5–25 mg range. DNA extraction from CM009 resulted in both insufficient nucleic acid yield and poor quality based on the absorbance ratio. Specimens CM006, CM007, CM008, and CM010, however, had ideal absorbance ratios to convey pure DNA extraction. Specimens CM011 – CM021 were similarly variable with respect to DNA yield. Specimens CM012, CM014, CM016 – CM020 indicated yield and absorbance values sufficient for PCR.

All lysed *C. testudinaria* specimens (CT054 – CT063, n = 10; collected January 2020) resulted in sufficient yield and adequate absorbance and were subjected to additional processing.

3.3.2. PCR and gel electrophoresis

PCR was performed for each of the three primer loci for all specimens. In total, 11 specimens of *C. manati* and 11 *C. testudinaria* were determined to have sufficient yield for one or more of the 16s, 28s, and COI primer loci to be analyzed in the initial sequence comparison, based on gel electrophoresis analysis. From these 22 specimens, 60 total samples were sequenced by Eton Bioscience, Inc. (San Diego, CA).

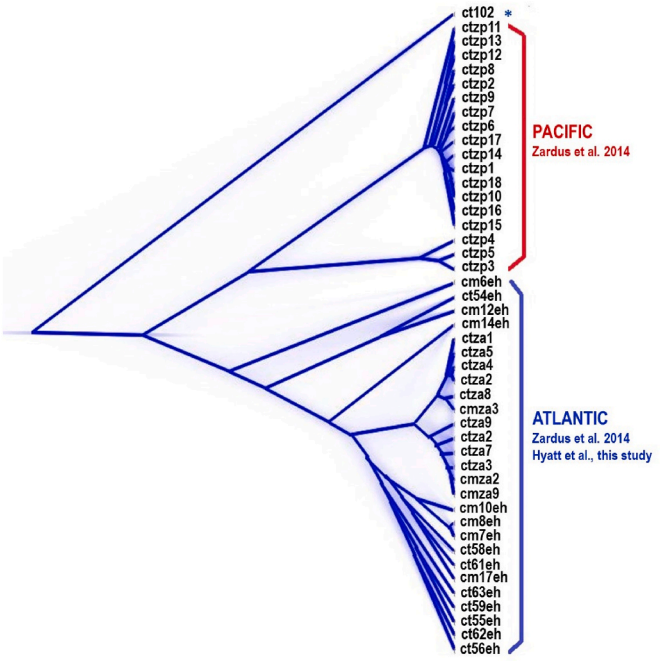

Fig. 6. Annotated maximum credibility consensus tree for presumed *Chelonibia testudinaria* (ct) and *C. manati* (cm) sequences from the Atlantic and Pacific Ocean basins, based on 571-bp region of COI generated with DensiTree software. The tree was constructed following Bayesian hierarchical clustering and tree annotation. n = 32 *C. testudinaria* and 8 *C. manati*. Asterisk indicates a single Atlantic turtle morphotype barnacle that did not correspond to Atlantic cluster.

3.3.3. BEAST analysis

For comparison at the 16s locus, the end likelihood mean of posterior probability summarizing the posterior distribution of phylogenetic trees for current samples was −6310.68 (±4.36, Var = 18.97). Posterior probability estimated a sample size (ESS) of 3360 after 10^7 MCMC iterations. Each statistic reported an ESS >200, indicating sufficient data to produce enough independent samples from the posterior distribution for each parameter (ESS range 514–6355) for the 12 statistics analyzed: Posterior probability, Likelihood, Prior, treeLikelihood, TreeHeight, YuleModel, birthrate, kappa, and frequency parameters 1–4); mean kappa (κ) = 1.74; and the highest posterior density (HPD) interval, representative of the shortest interval that contains 95% of the sampled values, was (−6319.70, −6303.12).

At the 28s site, the end likelihood mean of posterior probability summarizing the posterior distribution of phylogenetic trees for current samples was −6896.06 (±5.91, Var = 34.90) with posterior distribution ESS = 2915 after 10^7 MCMC iterations. As with the 16s results, each statistic reported a sufficient ESS (ESS range 579–4654) for the 12 statistics described above. Mean kappa (κ) at this locus was 1.08 with HPD was determined as (−6908.05, - 6885.23).

Comparing COI sequences, the end likelihood mean of posterior probability summarizing the posterior distribution of phylogenetic trees was −9887.02 (±3.73, Var = 13.94) with posterior distribution ESS = 2460 after 10^7 MCMC iterations. The ESS range exceeded minimum sufficiency values for all samples (329–9001). Mean kappa (κ) at this locus was 1.25 with HPD calculated as (−9894.51, −9877.19). Finally, the concatenated 16s-28s-COI analysis end likelihood mean of posterior

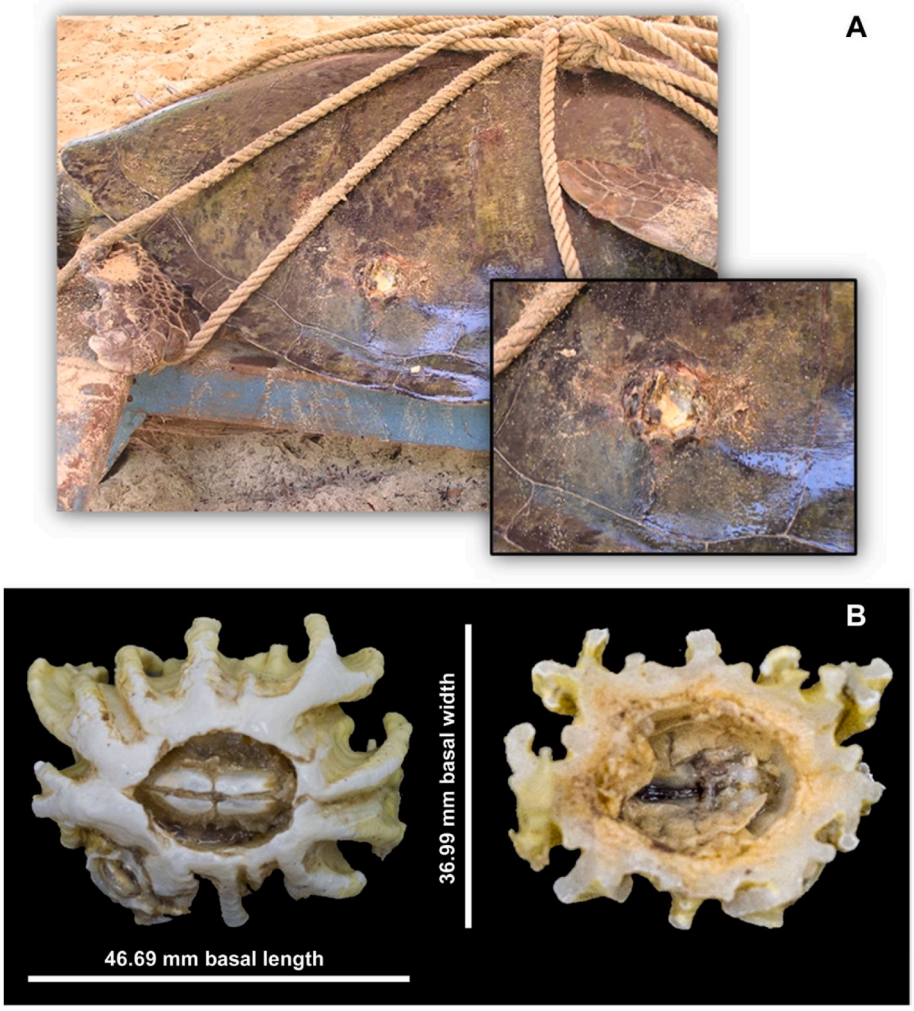

Fig. 7. (A) Post-extraction scar from embedded barnacle on lower right carapace of *C. mydas* individual MY549, collected June 01, 2005, in Zapatilla Cay, Panama. Closer image inset. Photos courtesy of P. and A. Meylan. (B) Images of presumed *C. manati* specimen CM038 (FWRI 77585) with clearly ridged external dorsal surface (left) and lack of invagination of inner wall or buttressing within test (right) that is characteristic of *C. manati*. Photos courtesy of Corinne Fuchs.

probability summarizing the posterior distribution of phylogenetic trees was −17715.62 (±2.70, Var = 7.31) with posterior probability ESS = 1663 after 10^6 MCMC iterations. ESS was of sufficient range (529–9000), mean kappa (κ) was 0.94, and HPD was (−17721.16, −17711.09).

A comparison of clades identified by BEAST maximum likelihood and SplitsTree network analysis showed consistency in output between the analytical methods. DensiTree output with all calculated trees is shown in Fig. 5A–D.

Results of the COI analysis with five *C. testudinaria* and five *C. manati* specimens from this study, as well as inclusion of Zardus et al. (2014) sequences, present geographic partitioning that conforms to expectations set by Zardus et al. (2014). Each of the ten specimens sequenced within this study clustered with the nine *C. testudinaria* and three *C. manati* from the western Atlantic and Caribbean, forming a separate population compared to the 18 Pacific *C. testudinaria* samples from Zardus et al. (2014) (Fig. 6).

4. Discussion

In this study, we assessed the morphological and genetic distinctiveness of barnacles derived from sea turtles and manatees. Our morphological analyses failed to provide unequivocal discrimination between barnacles collected from the two hosts, but substantial differentiation existed. We found strong evidence that one barnacle collected from a sea turtle fully matched the expected phenotype of barnacles collected from manatees. The genetic analyses were unable to identify meaningful distinction between the two groups, but were consistent with inter-oceanic clades as previously described by Zardus et al. (2014). The presumed *C. manati* specimen extracted from a green sea turtle in Zapatilla Cay, Panama (CM038, FWRI 70585; Fig. 7), adds to the prior literature documenting evidence that opposes the host-specific phenotypic plasticity hypothesis for unification of the *Chelonibia* species, and essentially rules out the implication of ecomorphic influence, such as soft-tissue specialization, by *C. manati* (Williams, 1972).

While our data indicate that the host-specific phenotypic plasticity hypothesis requires reevaluation, the present study is limited by the constraints that morphological data present when weighed against even minimal genetic comparison, as molecular data have been favored in some recent species classifications of barnacles (Chan et al., 2007; Cheang et al., 2013; Tsang et al., 2008; Zardus et al., 2014), although morphological character traits are still influential in contemporary cirriped species designations (Pérez-Losada et al., 2014). Thus, the cirral morphology and shell ratio data collected in the present study may be deemed insufficient to invalidate the hypothesis that phenotypic differences between the two *Chelonibia* species examined here illustrate distinct speciation rather than phenotypic plasticity.

Overall, the phylogenetic analyses based on discrete sequences and the concatenated sequence of multiple, independent genetic loci show that, while disparity exists in the degree of differentiation among the sequenced loci, collective genetic evidence appears to support conspecificity among the species. Despite apparent apomorphy, no genetic monophyly has been detected among barnacle specimens collected from manatee and turtle hosts.

The degree of variation in κ-values among the sites, however, is noteworthy. Recall, $\kappa = 1$ indicates gradual evolution; $\kappa < 1$ indicates proportionally more evolution in shorter branches; $\kappa > 1$ indicates that longer branches contribute proportionally more to trait evolution. $\kappa = 0$ indicates that the extent of evolutionary change is directly indicative of speciation events. For the discrete sequence comparisons, $\kappa > 1$ at all sites, though substantially higher at the 16s site than at 28s or COI. When concatenated, the combination of the three sites reduced this value to <1, indicative of higher evolutionary rates among the 10 specimens included in this comparison than the normal background mutation rate in animal cells.

In invertebrates, as in most animals, mtDNA evolves at a faster rate than nuclear DNA (nDNA) (Allio et al., 2017; Schindel and Miller, 2005). Allio et al. (2017) compared a variety of invertebrate taxa and found the mutation rate ratio of mtDNA over nDNA to be between 2 and 6. While lower than the general trend seen in vertebrates, the difference is still sufficient to allow mtDNA loci differentiation to provide suitable sites for species barcoding and identification (Allio et al., 2017). The more significant variation and higher κ in individual mtDNA sites (16s and COI) compared to nDNA (28s) in the current study conforms to this lower expected mutation rate. However, as the overall concatenated rate appears to be more rapid, the lower rate of differentiation in mutation rate demonstrated by Allio et al. (2017) may suggest that relying on mitochondrial genome phylogeny to differentiate invertebrate species may be less successful in demonstrating speciation than other species concepts, such as morphological, biological, or geographic differentiation.

The breadth of contrary evidence in the literature, as well as the magnitude of differentiation in phenotypic characteristics in the present study, warrant skepticism of conspecificity for *C. manati* and *C. testudinaria*. Both Cheang et al. (2013) and Zardus et al. (2014) used fewer than five genetic markers for their respective comparison studies that resulted in accepted lumping of the three species. Genetic comparisons with a more expansive set of loci and a broader range of sequence data would help elucidate whether the three taxa are, in fact, separate species as previously designated (Anderson, 1993; Darwin, 1854; Hayashi et al., 2013) until reclassification in 2014 (Zardus et al., 2014). In addition, there is need to determine if genetic information is appropriate for delineating barnacle species. In birds, for example, morphological variation generally supersedes molecular differentiation for species versus subspecies delineation, although disagreement persists (Barrowclough et al., 2016). Molecular analyses are not infallible, and in scenarios where morphological and molecular data conflict, an approach that combines methodologies may serve to better elucidate speciation (Sangster, 2014; Wiens, 2004). Further, it is important to employ rigor and incorporate a greater number of genetic loci and individuals in multiple studies to conclusively reclassify a species, especially within a broad, globally distributed taxonomic group, such as the genus *Chelonibia*. Results of the present study suggest that Balanomorph barnacle taxonomy, especially of endosymbiont species, requires further study, and that the hypothesis of phenotypic plasticity suggested by Cheang et al. (2013), and elaborated by Zardus et al. (2014), may be unsupported, at least within the two morphotypes we examined. Further, there may be evidence to support species-level geographic partitioning within *C. testudinaria*. Future experiments conducted in a controlled-flow laboratory environment may now be feasible given recent advances in lab-rearing techniques (Lane et al., 2021; Zardus and Lane, 2021). Because it is important to resolve endosymbiotic relationships of barnacle species with endangered coastal megafauna, it would be advantageous to determine if distinct morphologies are the result of phenotypic plasticity or inherent characteristics of separate *Chelonibia* species.

CRediT authorship contribution statement

Emily C. Hyatt: Writing – original draft, Methodology, Investigation, Formal analysis, Data curation, Conceptualization. **William K. Hayes:** Writing – review & editing, Methodology, Formal analysis, Data curation. **Stephen G. Dunbar:** Writing – review & editing, Supervision, Resources, Funding acquisition.

Declaration of competing interest

The authors declare that they have no known competing financial interests or personal relationships that could have appeared to influence the work reported in this paper.

Data availability

Data will be made available on request.

Acknowledgments

We thank the U.S. Geological Survey (St. Petersburg, FL); University of Florida Natural History Museum (Gainesville, FL); Florida Fish and Wildlife Research Institute (Gainesville, FL); Yale Peabody Museum (New Haven, CT); Georgia Sea Turtle Center (Jekyll Island, GA) for their specimen contributions and loans. This is Contribution No. 41 of the Marine Research Group (LLU), and Contribution No. 21 of ProTECTOR, Inc.

Appendix

List of specimens examined from the following museums: Florida Fish and Wildlife Research Institute (FWRI), University of Florida Natural History Museum (FLNHM), and Yale Peabody Museum (YPM).

Chelonibia testudinaria lots: FWRI 70586, FLNHM 6333, FLNHM 3188, FLNHM 3449, YPM IZ 76834, YPM IZ 77059.

Chelonibia manati lots: FWRI 70585, FLNHM 3796.

References

Allio, R., Donega, S., Galtier, N., Nabholz, B., 2017. Large variation in the ratio of mitochondrial to nuclear mutation rate across animals: implications for genetic diversity and the use of mitochondrial DNA as a molecular marker. Mol. Biol. Evol. 34, 2762–2772.

Anderson, D.T., 1993. Barnacles: Structure, Function, Development and Evolution. Springer Science & Business Media.

Arendt, J.D., 2006. The cellular basis for phenotypic plasticity of body size in Western Spadefoot toad (*Spea hammondi*) tadpoles: patterns of cell growth and recruitment in response to food and temperature manipulations. Biol. J. Linn. Soc. 88, 499–510.

Badrudeen, M., 2000. On the occurrence of the cirriped barnacle, *Chelonibia patula* (Ranzani) on the sea snake, *Hydrophis cyanocintus* (Daudin). Mar. Fish. Inf. Serv. Tech. Ext 164, 25.

Baldwin, J., 1896. A new factor in evolution. Am. Nat. 30.

Barrowclough, G.F., Cracraft, J., Klicka, J., Zink, R.M., 2016. How many kinds of birds are there and why does it matter? PLoS One 11, e0166307.

Blackburne, B.P., Whelan, S., 2012. Measuring the distance between multiple sequence alignments. Bioinformatics 28, 495–502.

Bouckaert, R.R., Heled, J., 2014. DensiTree 2: Seeing Trees through the Forest. BioRxiv, 012401.

Bryant, D., Moulton, V., 2004. Neighbor-net: an agglomerative method for the construction of phylogenetic networks. Mol. Biol. Evol. 21, 255–265.

Butchart, S.H., Walpole, M., Collen, B., Van Strien, A., Scharlemann, J.P., Almond, R.E., Watson, R., 2010. Global biodiversity: indicators of recent declines. Science 328 (5982), 1164–1168.

Chan, B.K.K., Garm, A., Høeg, J.T., 2008. Setal morphology and cirral setation of thoracican barnacle cirri: adaptations and implications for thoracican evolution. J. Zool. 275 (3), 294–306.

Chan, B.K.K., Tsang, L., Ma, K., Hsu, C.H., Chu, K., 2007. Taxonomic revision of the acorn barnacles *Tetraclita japonica* and *Tetraclita formosana* (Crustacea: Cirripedia) in East Asia based on molecular and morphological analyses. Bull. Mar. Sci. 81, 101–113.

Cheang, C.C., Tsang, L.M., Chu, K.H., Cheng, I.J., Chan, B.K.K., 2013. Host-specific phenotypic plasticity of the turtle barnacle *Chelonibia testudinaria*: a widespread generalist rather than a specialist. PLoS One 8, e57592.
Cintrón-de Jesús, J., 2000. Barnacles associated with marine vertebrates in Puerto Rico and Florida. University of Puerto Rico, Mayagüez Campus.
Collareta, A., Bianucci, G., 2021. The occurrence of the coronuloid barnacle *Chelonibia* Leach, 1817 as an encruster on mammalian bone in the central Mediterranean Sea. Acta Adriat. 62, 83–92.
Coordinators, N.R., 2015. Database resources of the national center for biotechnology information. Nucleic Acids Res. 43, D6–D17.
Crisp, D., Southward, A.J., 1961. Different types of cirral activity of barnacles. Phil. Trans. Roy. Soc. Lond. B Biol. Sci. 243, 271–307.
Darroch, J.N., Mosimann, J.E., 1985. Canonical and principal components of shape. Biometrika 72, 241–252.
Darwin, C., 1854. The Balanidae, the Verrucidae, Etc., vol. 2. The Ray Society, London.
Dean, R., 2010. Delicacy or desperation? Eating peduncular barnacles in Neolithic Portugal. J. Ethnobiol. 30, 80–91.
Dress, A.W., Huson, D.H., 2004. Constructing splits graphs. IEEE ACM Trans. Comput. Biol. Bioinf 1, 109–115.
Edgar, R.C., 2004. MUSCLE: a multiple sequence alignment method with reduced time and space complexity. BMC Bioinf. 5, 1–19.
Folmer, O., Black, M., Hoeh, W., Lutz, R., Vrijenhoek, R., 1994. DNA primers for amplification of mitochondrial cytochrome c oxidase subunit I from diverse metazoan invertebrates. Mol. Mar. Biol. Biotechnol. 3, 294–299.
Frazier, J., Margaritoulis, D., 1990. The occurrence of the barnacle, *Chelonibia patula* (Ranzani, 1818), on an inanimate substratum (Cirripedia, Thoracica). Crustaceana 59, 213–218.
Frick, M.G., Pfaller, J.B., 2013. Sea turtle epibiosis. Biology of Sea Turtles 3, 399.
Frick, M.G., Slay, C.K., 2000. *Caretta caretta* (loggerhead sea turtle) epizoans. Herpetol. Rev. 31, 102–103.
Geierman, C., 2007. Barnacle feeding: comparing cirral anatomy, feeding behavior, Reynolds numbers, and cirral fan leakiness across three size classes of three species of common acorn barnacles. University of Oregon, Eugene, OR.
Gibert, P., Moreteau, B., David, J., 2004. Phenotypic plasticity of body pigmentation in *Drosophila melanogaster*: genetic repeatability of quantitative parameters in two successive generations. Heredity 92, 499–507.
Hasegawa, M., Kishino, H., Yano, T.A., 1985. Dating of the human-ape splitting by a molecular clock of mitochondrial DNA. J. Mol. Evol. 22, 160–174.
Hayashi, R., Chan, B.K.K., Simon-Blecher, N., Watanabe, H., Guy-Haim, T., Yonezawa, T., Levy, Y., Shuto, T., Achituv, Y., 2013. Phylogenetic position and evolutionary history of the turtle and whale barnacles (Cirripedia: Balanomorpha: Coronuloidea). Mol. Phylogenet. Evol. 67, 9–14.
Hernandez, C.E., Rodríguez-Serrano, E., Avaria-Llautureo, J., Inostroza-Michael, O., Morales-Pallero, B., Boric-Bargetto, D., Canales-Aguirre, C.B., Marquet, P.A., Meade, A., 2013. Using phylogenetic information and the comparative method to evaluate hypotheses in macroecology. Methods Ecol. Evol. 4, 401–415.
Hoch, M.J., 2011. Effects of crowding and wave exposure on cirrus morphology of the acorn barnacle, *Semibalanus balanoides*. J. Crustac Biol. 31, 401–405.
Holm, E.R., 2012. Barnacles and biofouling. Integr. Comp. Biol. 52, 8.
Huson, D.H., Bryant, D., 2006. Application of phylogenetic networks in evolutionary studies. Mol. Biol. Evol. 23, 254–267.
Huson, D.H., Bryant, D., 2012. User Manual for SplitsTree4 V4, vol. 12, p. 6.
Ingels, J., Valdes, Y., Pontes, L.P., Silva, A.C., Neres, P.F., Corrêa, G.V., Silver-Gorges, I., Fuentes, M.M., Gillis, A., Hooper, L., 2020. Meiofauna life on loggerhead sea turtles-diversely structured abundance and biodiversity hotspots that challenge the meiofauna paradox. Diversity 12, 203.
IUCN, 2022. The IUCN Red List of Threatened Species.
Jinbo, U., Kato, T., Ito, M., 2011. Current progress in DNA barcoding and future implications for entomology. Entomol. Sci. 14, 107–124.
Jonsson, P.R., Wrange, A.-L., Lind, U., Abramova, A., Ogemark, M., Blomberg, A., 2018. The barnacle *Balanus improvisus* as a marine model-culturing and gene expression. JoVE, e57825.
Karthika, K., Anand, P., Seena, S., Shibu Vardhanan, Y., 2022. Wing phenotypic plasticity, quantitative genetics, modularity, and phylogenetic signal analysis revealed the niche partitioning in two fruit fly species, *Bactrocera dorsalis* and *Zeugodacus cucurbitae*. Int. J. Trop. Insect Sci. 42, 1487–1504.
Key Jr., M.M., Volpe, J.W., Jeffries, W.B., Voris, H.K., 1997. Barnacle fouling of the blue crab *Callinectes sapidus* at Beaufort, North Carolina. J. Crustac Biol. 17, 424–439.
Lance, R.F., Kennedy, M.L., Leberg, P.L., 2000. Classification bias in discriminant function analyses used to evaluate putatively different taxa. J. Mammal. 81 (1), 245–249.
Lane, Z.M., McElroy, E.J., Kendrick, M.R., Zardus, J.D., 2021. Experimental demonstration of exclusively passive feeding in the sea-turtle barnacle *Chelonibia testudinaria* (Linnaeus, 1758)(Cirripedia: Coronulidae). J. Crustacean Biol. 41 (4), ruab053.
Larkin, M.A., Blackshields, G., Brown, N.P., Chenna, R., McGettigan, P.A., McWilliam, H., Valentin, F., Wallace, I.M., Wilm, A., Lopez, R., 2007. Clustal W and clustal X version 2.0. Bioinformatics 23, 2947–2948.
Li, N.K., Denny, M.W., 2004. Limits to phenotypic plasticity: flow effects on barnacle feeding appendages. Biol. Bull. 206, 121–124.
López, B.A., Ramírez, R.P., Guaitro, S.Y., López, D.A., 2010. Interspecific differences in the phenotypic plasticity of intertidal barnacles in response to habitat changes. J. Crustac Biol. 30, 357–365.
Maciejeski, J., 2008. Cirral length and wave exposure in the barnacle *Semibalanus cariosus*.
Marchinko, K.B., 2003. Dramatic phenotypic plasticity in barnacle legs (*Balanus glandula* Darwin): magnitude, age dependence, and speed of response. Evolution 57, 1281–1290.
Marchinko, K.B., Palmer, A.R., 2003. Feeding in flow extremes: dependence of cirrus form on wave-exposure in four barnacle species. Zoology 106, 127–141.
Michener, C.D., Sokal, R.R., 1957. A quantitative approach to a problem in classification. Evolution 11, 130–162.
Mignucci-Giannoni, A.A., Beck, C.A., Montoya-Ospina, R.A., Williams Jr., E.H., 1999. Parasites and commensals of the West Indian manatee from Puerto Rico. Skin 87812, 87803, 87812.
Monroe, R., Garrett, R., 1979. *Chelonibia testudinaria* (Cirripedia, Coronulidae) on *Crocodylus porosus* Schneider, a new host record. Crustaceana 36, 108-108.
Mosimann, J.E., 1970. Size allometry: size and shape variables with characterizations of the lognormal and generalized gamma distributions. J. Am. Stat. Assoc. 65, 930–945.
Mosimann, J.E., James, F.C., 1979. New statistical methods for allometry with application to Florida red-winged blackbirds. Evolution 444–459.
Needleman, S.B., Wunsch, C.D., 1970. A general method applicable to the search for similarities in the amino acid sequence of two proteins. J. Mol. Biol. 48, 443–453.
Newman, W.A., Abbott, D.P., 1980. Cirripedia: the barnacles. Intertidal invertebrates of. California 200, pp. 504–535.
Nifong, J.C., Frick, M.G., 2011. First record of the American alligator (*Alligator mississippiensis*) as a host to the sea turtle barnacle (*Chelonibia testudinaria*). SE. Nat. 10, 557–560.
Nussey, D.H., Postma, E., Gienapp, P., Visser, M.E., 2005. Selection on heritable phenotypic plasticity in a wild bird population. Science 310, 304–306.
Pagel, M., 1999. Inferring the historical patterns of biological evolution. Nature 401, 877–884.
Pentinsaari, M., Salmela, H., Mutanen, M., Roslin, T., 2016. Molecular evolution of a widely-adopted taxonomic marker (COI) across the animal tree of life. Sci. Rep. 6, 1–12.
Pérez-Losada, M., Høeg, J.T., Simon-Blecher, N., Achituv, Y., Jones, D., Crandall, K.A., 2014. Molecular phylogeny, systematics and morphological evolution of the acorn barnacles (Thoracica: Sessilia: Balanomorpha). Mol. Phylogenet. Evol. 81, 147–158.
Pétavy, G., Morin, J., Moreteau, B., David, J., 1997. Growth temperature and phenotypic plasticity in two *Drosophila* sibling species: probable adaptive changes in flight capacities. J. Evol. Biol. 10, 875–887.
Pfennig, D.W., Wund, M.A., Snell-Rood, E.C., Cruickshank, T., Schlichting, C.D., Moczek, A.P., 2010. Phenotypic plasticity's impacts on diversification and speciation. Trends Ecol. Evol. 25, 459–467.
Pigliucci, M., Murren, C.J., Schlichting, C.D., 2006. Phenotypic plasticity and evolution by genetic assimilation. J. Exp. Biol. 209, 2362–2367.
Pilsbry, H.A., 1916. The sessile barnacles (Cirripedia) contained in the collections of the U.S. National Museum; including a monograph of the American species. Bulletin of the United States National Museum, pp. 1–366.
Polyanovsky, V.O., Roytberg, M.A., Tumanyan, V.G., 2011. Comparative analysis of the quality of a global algorithm and a local algorithm for alignment of two sequences. Algorithm Mol. Biol. 6, 1–12.
Posada, D., Crandall, K.A., 1998. MODELTEST: testing the model of DNA substitution. Bioinformatics 14, 817–818.
Prince, A.M., Andrus, L., 1992. PCR: how to kill unwanted DNA. Biotechniques 12, 358–360.
Rambaut, A., Drummond, A.J., Xie, D., Baele, G., Suchard, M.A., 2018. Posterior summarization in Bayesian phylogenetics using Tracer 1.7. Syst. Biol. 67, 901.
Rawson, P., Macnamee, R., Frick, M., Williams, K., 2003. Phylogeography of the coronulid barnacle, *Chelonibia testudinaria*, from loggerhead sea turtles, *Caretta caretta*. Mol. Ecol. 12, 2697–2706.
Rice, P., Longden, I., Bleasby, A., 2000. EMBOSS: The European molecular biology open software suite. Trends Genet. 16, 276–277.
Rivera, A., Gelcich, S., García-Florez, L., Alcázar, J.L., Acuña, J.L., 2014. Co-management in Europe: insights from the gooseneck barnacle fishery in Asturias, Spain. Mar. Pol. 50, 300–308.
Ross, A., Jackson, C.G., 1972. Barnacle fouling of the ornate diamondback terrapin, *Malaclemys terrapin macrospilota*. Crustaceana 22, 203–205.
Saitou, N., Nei, M., 1987. The neighbor-joining method: a new method for reconstructing phylogenetic trees. Mol. Biol. Evol. 4, 406–425.
Sangster, G., 2014. The application of species criteria in avian taxonomy and its implications for the debate over species concepts. Biol. Rev. 89, 199–214.
Scheiner, S.M., Levis, N.A., 2021. The loss of phenotypic plasticity via natural selection: genetic assimilation. In: Phenotypic Plasticity & Evolution. CRC Press, pp. 161–181.
Schindel, D.E., Miller, S.E., 2005. *Success stories in implementation of the programmes of work on dry and sub-humid lands and the global taxonomy initiative: DNA Barcoding and the Consortium for the Barcode of Life*. Paper presented at the 11th meeting of the Subsidiary Body on Scientific, Technical, and Technological Advice. Montreal, Canada.
Schneider, C.A., Rasband, W.S., Eliceiri, K.W., 2012. NIH Image to ImageJ: 25 years of image analysis. Nat. Methods 9, 671–675.
Seigel, R.A., 1983. Occurrence and effects of barnacle infestations on diamondback terrapins (*Malaclemys terrapin*). Am. Midl. Nat. 34–39.
Shahdadi, A., Sari, A., Naderloo, R., 2014. A checklist of the barnacles (Crustacea: Cirripedia: Thoracica) of the Persian Gulf and Gulf of Oman with nine new records. Zootaxa 3784, 201–223.
Sloan, K., Zardus, J.D., Jones, M.L., 2014. Substratum fidelity and early growth in *Chelonibia testudinaria,* a turtle barnacle especially common on debilitated loggerhead (*Caretta caretta*) sea turtles. Bull. Mar. Sci. 90, 581–597.

Söding, J., 2005. Protein homology detection by HMM–HMM comparison. Bioinformatics 21, 951–960.
Spivey, H.R., 1988. Shell morphometry in barnacles: quantification of shape and shape change in *Balanus*. J. Zool. 216, 265–294.
Stamatakis, A., 2006. Phylogenetic models of rate heterogeneity: a high performance computing perspective. In: Paper Presented at: Proceedings of the 20th Institute of Electrical and Electronics Engineers (IEEE) International Parallel & Distributed Processing Symposium. IEEE.
Suchard, M.A., Lemey, P., Baele, G., Ayres, D.L., Drummond, A.J., Rambaut, A., 2018. Bayesian phylogenetic and phylodynamic data integration using BEAST 1.10. Virus Evol. 4, vey016.
Swinehart, D.F., 1962. The beer-lambert law. J. Chem. Educ. 39, 333.
Todd, P.A., 2008. Morphological plasticity in scleractinian corals. Biol. Rev. 83, 315–337.
Trivedi, S., Aloufi, A.A., Ansari, A.A., Ghosh, S.K., 2016. Role of DNA barcoding in marine biodiversity assessment and conservation: an update. Saudi J. Biol. Sci. 23, 161–171.
Tsang, L.M., Chan, B.K., Ma, K.Y., Chu, K.H., 2008. Genetic differentiation, hybridization and adaptive divergence in two subspecies of the acorn barnacle *Tetraclita japonica* in the northwestern Pacific. Mol. Ecol. 17, 4151–4163.
Vallini, C., Rubini, S., Tarricone, L., Mazziotti, C., Gaspari, S., 2011. Unusual stranding of live, small, debilitated loggerhead turtles along the northwestern Adriatic coast. Mar. Turt. Newsl. 131, 25–28.
Waddington, C.H., 1953. Genetic assimilation of an acquired character. Evolution 118–126.
Waddington, C.H., 1956. Genetic assimilation of the bithorax phenotype. Evolution 1–13.
Wells, H.W., 1966. Barnacles of the northeastern Gulf of Mexico. Q. J. Fla. Acad. Sci. 29, 81–95.
West-Eberhard, M.J., 2003. Developmental Plasticity and Evolution. Oxford University Press.
Wiens, J.J., 2004. The role of morphological data in phylogeny reconstruction. Syst. Biol. 53, 653–661.
Williams, E.E., 1972. The origin of faunas. Evolution of lizard congeners in a complex island fauna: a trial analysis. In: Dobzhansky, T., Hecht, M.K., Steere, W.C. (Eds.), Evolutionary Biology. Springer, New York, NY, pp. 47–89.
Zardus, J.D., Lake, D.T., Frick, M.G., Rawson, P.D., 2014. Deconstructing an assemblage of "turtle" barnacles: species assignments and fickle fidelity in *Chelonibia*. Mar. Biol. 161, 45–59.
Zardus, J.D., Lane, Z.M., 2021. Revolutions in rearing barnacles: rotating flow and substratum for culturing larvae and adults. Bullet. Marine Sci. 97 (1), 143–162.
Zhao, Y., Zhang, W.Y., Wang, R.L., Niu, D.L., 2020. Divergent domains of 28S ribosomal RNA gene: DNA barcodes for molecular classification and identification of mites. Parasites Vectors 13, 1–12.